

Proton Spin Lattice Relaxation in Vinylidene Fluoride/ Trifluoroethylene Copolymer I. Vinylidene Fluoride 72 mol% Copolymer

Fumiaki ISHII and Akira ODAJIMA

*Department of Applied Physics, Faculty of Engineering,
Hokkaido University, Sapporo 060, Japan*

(Received December 19, 1985)

ABSTRACT: The proton spin lattice relaxation times T_1 of drawn films of a VDF/TrFE copolymer (VDF 72 mol%) were measured for various values of γ , which was the angle between the magnetic field and the draw direction of the film, and for different Larmor frequencies ω , over a temperature range from -23 to 130°C . Three kinds of T_1 relaxation processes were observed below the Curie temperature (T_c), around T_c , and at a certain temperature in the paraelectric phase. The curve of $\ln T_1$ against reciprocal temperature $1/T$ was linear for the relaxation process in the paraelectric phase. The T_1 became larger as the frequency ω and the angle γ increased.

The formulation of T_1 in the paraelectric phase for the oriented copolymer was derived, using the non-exponential correlation function which describes a one dimensional diffusion motion of conformational defects along the chain. The existence of the 1-D diffusion motion of the conformational defect was confirmed by a reasonable agreement between the theoretical and experimental results.

KEY WORDS Nuclear Spin Lattice Relaxation / Vinylidene Fluoride / Trifluoroethylene Copolymer / Non-Exponential Correlation Function / Long-Time $\tau^{-1/2}$ Tails / Paraelectric Phase / 1-D Diffusion Motion / Conformational Defects /

The vinylidene fluoride (VDF) and trifluoroethylene (TrFE) copolymer is a ferroelectric polymer which exhibits the transition from ferro- to paraelectric phase. The Curie temperature, T_c and the transition behavior in the copolymer depend greatly on the VDF content.¹ One of the features of the ferroelectric phase transition in this copolymer is that its mechanism is closely related to the change of the chain conformation from the all-*trans* form in the ferroelectric phase to the *gauche* form with the statistical combination of the TG^\pm and T_3G^\pm rotational isomers in the paraelectric phase.¹ In a previous paper,² the temperature dependence of the NMR second moment in the drawn film of P(VDF₇₂/TrFE₂₈) with VDF (72 mol%) was measured for various values of

γ , which is the alignment angle between the draw direction of the film and the static magnetic field, and the motional modes of the chain in both phases were discussed. The second moment, $\langle\Delta H^2\rangle$, decreased in four stages in the temperature region between 23 and 130°C . The decrement of the second moment, $\delta\langle\Delta H^2\rangle$ in each stage was dependent on the angle γ and gave rise to the concave curve against γ . The concave curve for the transition region was explained by the chain motion accompanying the conformational change from the all-*trans* form to the *gauche* form. At a higher temperature in the *para*-electric phase, the γ -dependence of the NMR line width was interpreted by the local field modulated by a one-dimensional (1-D) diffusion motion of the conformational defects along

the chain, of which the correlation function is dependent on time τ by the "one-half" law.^{2,3} The "long-time $\tau^{-1/2}$ tails" means that interchain interactions are extremely weak in comparison with intrachain interactions in the paraelectric phase.

A simple model of a one-dimensional "defect" diffusion has been elaborated by Hunt and Powles.⁴ The non-exponential correlation function in this model explains the concave curve of the spin-lattice relaxation time T_1 against reciprocal temperature (T^{-1}) and the Bloch decay shape for *n*-isobutyl bromide, which could not be explained by the earlier analysis⁵ using the exponential correlation function.

Bloembergen⁶ has assumed the exponential correlation functions of the local field and derived the formulas of T_1 of an isolated dipole pair rotating about a single fixed axis for two simple models: (i) random jumps between three equilibrium positions of the azimuthal angle ψ , and (ii) the statistical oscillation in the angle ψ at time t with the Gaussian distribution $g(\psi, t)$. The theoretical T_1 for each model is strongly dependent on the angle γ between the axis of rotation and the magnetic field, and the angle β between its axis and the vector \vec{r}_{12} of the dipole pair.

In this paper, we report spin-lattice relaxation studies of the drawn films of P(VDF₇₂/TrFE₂₈), by using the pulse NMR technique. The T_1 measurements of molecular relaxations are compared with the published data of dielectric,⁷ DSC,⁷ and NMR line width² studies. It is shown that the non-exponential correlation function in the "defect" diffusion⁴ is the correlation function applicable for the local field in an isolated spin pair modulated by the 1-D diffusion motion of the conformation defect. A formula for T_1 in an anisotropic system for the non-exponential correlation function is obtained as a function of the resonance frequency, the angles of γ and β , and the correlation time of the local field, on the basis of Bloembergen's theory.

Furthermore, we verify the existence of the 1-D diffusion motion in the paraelectric phase by showing a reasonable agreement between the theory and the experimental results.

THEORY

Nuclear Spin-Lattice Relaxation Due to a One-Dimensional Diffusion Motion of the Conformational Defect

Correlation Function

Let us apply Hunt and Powles's theory⁴ to a 1-D diffusion motion of the conformational defect along a chain in the paraelectric phase described in the previous paper.² We assume that the conformational defect distributes randomly in the chain and that the nearest defect is at a distance l from an isolated spin pair in the chain at a time $\tau = 0$. If $P(\tau)$ is the probability that the conformational defect reaches the isolated spin pair in the time τ , the correlation function of the local field in an isolated spin pair modulated by the 1-D diffusion motion of the conformational defect equals the probability of the defect not having arrived after time τ , that is, $\varphi_D(\tau) = 1 - P(\tau)$. Hunt and Powles⁴ obtained the correlation function $\varphi_D(\tau)$ as

$$\varphi_D(\tau) = \exp\left(\frac{\tau}{\tau_D}\right) \left\{ 1 - \operatorname{erf}\left(\left(\frac{\tau}{\tau_D}\right)^{1/2}\right) \right\} \quad (1)$$

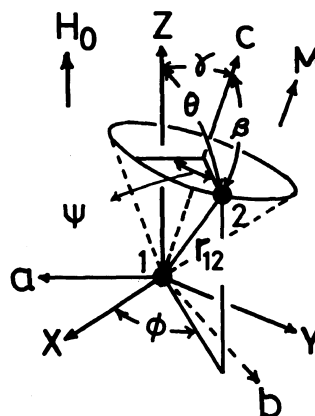


Figure 1. Relation between the laboratory coordinate (x, y, z) and the crystal coordinate (a, b, c).

where $\text{erf}(\tau/\tau_D)$ is the error function. τ_D is the correlation time and is defined as $\tau_D = l_d^2/D$, where $2 \cdot l_d$ is the mean distance between conformational defects and D is the diffusion coefficient.

For $\tau_D \ll \tau$, eq 1 is approximated by*

$$\varphi_D(\tau) = \frac{1}{2} \tau_D^{1/2} \tau^{-1/2} \quad (2)$$

Equation 2 is equivalent to the correlation function of the local magnetic field described in the previous paper.^{2,3}

Anisotropy

Since the c -axis orientation coefficient for the drawn film of P(VDF₇₂/TrFE₂₈) is 0.98,² the c -axis may be preferentially oriented to the draw direction, M -axis. Figure 1 shows the relationship between the laboratory coordinate (x, y, z) and the crystalline coordinate (a, b, c) , in which the c -axis is parallel to M -axis, and the angles β and $\psi(t)$ are, respectively, the polar and azimuthal angles of the vector $\vec{r}_{12}(t)$ in an isolated spin pair. In general, Hamiltonian of the nuclear magnetic dipole-dipole interaction, $H_d(t)$, in the two spin (1 and 2) system under the static magnetic field H_0 is represented by

$$H_d(t) = \sum_{p=-2}^2 F_{12}^{(-p)}(t) A_{12}^{(p)} \quad (3)$$

$$F_{12}^{(0)}(t) = 1/2 K (1 - 3 \cos^2 \theta_{12}) \equiv P_0^{(2)}(\theta_{12})$$

$$F_{12}^{(\pm 1)}(t) = -3/2 K \sin^2 \theta_{12} \cos \theta_{12} \exp(\pm i \phi_{12}) \\ \equiv P_{\pm 1}^{(2)}(\theta_{12}, \phi_{12})$$

$$F_{12}^{(\pm 2)}(t) = -3/4 K \sin^2 \theta_{12} \exp(\pm 2i \phi_{12}) \\ \equiv P_{\pm 2}^{(2)}(\theta_{12}, \phi_{12}) \quad (4a) \\ K = \gamma_1 \gamma_2 n^2 r_{12}^{-3}$$

and

$$A_{12}^{(0)} = I_1 I_2 - 3 I_1^z I_2^z \\ A_{12}^{(\pm 1)} = I_1^z I_2^{\pm} + I_1^{\pm} I_2^z \\ A_{12}^{(\pm 2)} = I_1^{\pm} I_2^{\pm} \quad (4b)$$

where $\theta_{12}(t)$ and $\phi_{12}(t)$ are, respectively, the polar and azimuthal angles of $\vec{r}_{12}(t)$ in the (x, y, z) coordinate. The T_1 in the two-spin system obtained by Bloembergen⁶ is given by

$$\frac{1}{T_1} = 2(W^{(1)}(\omega) + W^{(2)}(2\omega)) \quad (5)$$

If $|m_1\rangle$ and $|m_2\rangle$ are two eigenstates of the unperturbed Hamiltonian with the corresponding energy E_1 and E_2 , the transition probability per unit time between these two states, $W^{(q)}(q\omega)$ is expressed as

$$W^{(q)}(q\omega) = \frac{q}{2\hbar^2} \langle A_{12}^{(p)} \rangle \int_{-\infty}^{\infty} \langle F^{(p)}(0) F^{(-p)}(\tau) \rangle e^{iq\omega\tau} d\tau \\ = \frac{q}{2\hbar^2} \langle A_{12}^{(p)} \rangle \langle |F^{(p)}(0)|^2 \rangle \\ \times \int_{-\infty}^{\infty} \varphi_{12}^{(q)}(\tau) e^{iq\omega\tau} d\tau, \quad q = |p|. \quad (6a)$$

* $\{1 - \text{erf}(x)\}$ is represented by the asymptotic expansion as

$$1 - \text{erf}(x) \sim \int_x^{\infty} e^{-t^2} dt - e^{-x^2} \sum_{n=0}^{\infty} (-2)^n \frac{(2n-1)!!}{2^{n+1} x^{2n+1}}$$

Since the first term for $n=0$ on the right side is dominant for $x \rightarrow \infty$, the error function takes the simpler form

$$\text{erf}(x) = 1 - \frac{1}{2x} \exp(-x^2) \quad (x \rightarrow \infty)$$

Therefore, if $x = (\tau/\tau_D)^{1/2}$, eq 1 is approximated by

$$\varphi_D(\tau) = \frac{1}{2} \tau_D^{1/2} \tau^{-1/2} \quad [\tau/\tau_D \rightarrow \infty]$$

where

$$\varphi^{(q)}(\tau) = \langle e^{\pm iq\phi(0)} e^{\pm iq\phi(\tau)} \rangle \quad (6b)$$

$$\langle A_{12}^{(p)} \rangle = |\langle m_1 | A_{12}^{(p)} | m_2 \rangle|^2$$

and ω is the angular resonance frequency.

Conformational defects emerged thermally in the chain move along the chain axis as the 1-D diffusion motion.² The transition probability, $W^{(q)}(q\omega)$, is calculated by assuming that $H_d(t)$ is modulated by the 1-D diffusion motion and

$$\varphi_{12}^{(1)}(\tau) = \varphi_{12}^{(2)}(\tau) = \varphi_D(\tau) \quad (7)$$

Then, T_1 of the 1-D diffusion motion is represented by**

$$\begin{aligned} \frac{1}{T_1} = & \frac{9}{8} \frac{\gamma^4 \hbar^2}{\gamma_{12}^6} \left\{ \left[\sin^2 \beta \cos^2 \beta (4 \cos^4 \gamma - 3 \cos^2 \gamma + 1) \right. \right. \\ & \left. \left. + \frac{1}{4} \sin^4 \beta (1 - \cos^4 \gamma) \right] \frac{\tau_D}{1 + \omega^2 \tau_D^2} \right. \\ & \times \left(\frac{1 + \omega \tau_D}{\sqrt{2\omega \tau_D}} - 1 \right) \\ & + \left[2 \sin^2 \beta \cos^2 \beta (1 - \cos^4 \gamma) \right. \\ & \left. + \frac{1}{8} \sin^4 \beta (1 + 6 \cos^2 \gamma + \cos^4 \gamma) \right] \\ & \left. \times \frac{\tau_D}{1 + 4\omega^2 \tau_D^2} \left(\frac{1 + 2\omega \tau_D}{2\sqrt{\omega \tau_D}} - 1 \right) \right\} \quad (8) \end{aligned}$$

EXPERIMENTAL

The sample used was the film of a random

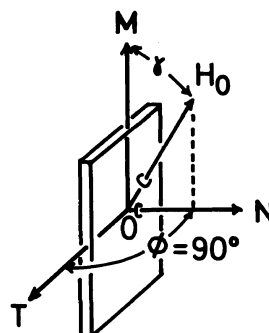


Figure 2. TNM coordinate fixed in the drawn film. The direction of the magnetic field H_0 is specified by the alignment angle γ .

copolymer P(VDF₇₂/TrFE₂₈) supplied by the Daikin Kogyo Co., Ltd. The film was drawn $\times 4.5$ uniaxially at room temperature and annealed at 135°C for 20 h. Its final draw ratio was 3.8 and its thickness was 97 μm .

The measurement of proton magnetic resonance was carried out by a Bruker SXP 4-100 NMR spectrometer operating mainly with the resonance frequencies of 20, 36, and 90 MHz over a temperature range from -23 to 130°C. The films were packed in the glass sample holder of a square pillar suspended from a goniometer head to permit a continuous variation of γ . Figure 2 illustrates the TNM coordinates fixed to the sample. The magnetic field H_0 applied was in the plane containing the drawn axis M and the normal axis N . The alignment angle γ was varied to 0, 45, and 90° at temperatures ranging from -23 to 130°C. Free induction decay of proton magnetization could be observed from 5-10 μs after the 2.9 μs 90° pulse. The null

** In the derivation of eq 8, the calculation of $\langle |F^{(p)}(0)|^2 \rangle$ is made under transformation from the spherical harmonics $P_m^{(2)}(\beta_{12}, \psi_{12})$ to $P_m^{(2)}(\theta_{12}, \phi_{12})$ ⁸ as follows:

$$P_m^{(2)}(\theta_{12}, \phi_{12}) = \sum_{m'=-2}^2 D_{mm'}^{(2)}(0, \gamma, 0) P_{m'}^{(2)}(\beta_{12}, \psi_{12}), \quad (m=p)$$

where $D_{mm'}^{(2)}(0, \gamma, 0)$ is Wigner's rotation matrix. Wigner's matrix has the following functional dependence on the Euler angle γ :

$$D_{mm'}^{(2)}(0, \gamma, 0) = \left[\frac{(2+m')!(2-m)!}{(2+m)!(2-m')} \right] \left(\cos \frac{\gamma}{2} \right)^{m+m'} \left(\sin \frac{\gamma}{2} \right)^{m-m'} P_{1-m}^{(m-m', m+m')}(\cos \gamma)$$

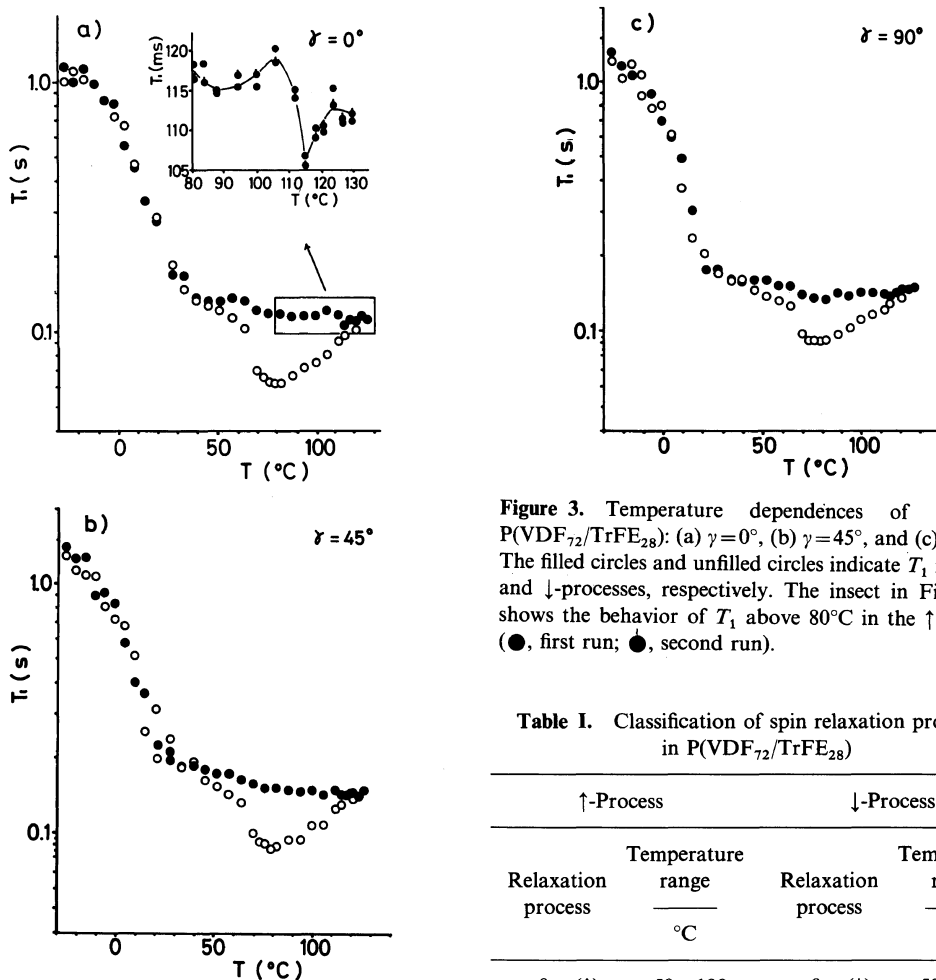


Figure 3. Temperature dependences of T_1 for P(VDF₇₂/TrFE₂₈): (a) $\gamma = 0^\circ$, (b) $\gamma = 45^\circ$, and (c) $\gamma = 90^\circ$. The filled circles and unfilled circles indicate T_1 in the \uparrow - and \downarrow -processes, respectively. The inset in Figure 3a shows the behavior of T_1 above 80°C in the \uparrow process (\bullet , first run; \bullet , second run).

Table I. Classification of spin relaxation processes in P(VDF₇₂/TrFE₂₈)

\uparrow -Process		\downarrow -Process	
Relaxation process	Temperature range °C	Relaxation process	Temperature range °C
β (\uparrow)	50–100	β (\downarrow)	50–65
α_t (\uparrow)	110–120	α_t (\downarrow)	70–95
α'_b (\downarrow)	120–130	α'_b (\downarrow)	95–130

method of a $180^\circ\text{C}-\tau-90^\circ$ pulse sequence was used to determine T_1 with a precision of 0.5–0.8%.

EXPERIMENTAL RESULTS

Figures 3a, b, and c show the $\ln T_1$ vs. T curves of P(VDF₇₂/TrFE₂₈) for $\gamma = 0, 45,$ and 90° , respectively. The filled and unfilled circles indicate the values of T_1 for the temperature rise from -23 to 130°C (\uparrow) and for its fall from 130 to -23°C (\downarrow), respectively. Here, the temperature rising and falling in a thermal cycle are taken as \uparrow - and \downarrow -processes, respectively. In the \uparrow -process, the T_1 's plotted against T give

the concave curves in two temperature ranges from 50 to 100°C (\uparrow) and from 110 to 120°C (\uparrow), in which the relaxation processes are referred to as β (\uparrow) and α_t (\uparrow), respectively. (Hereafter, the same notations as those in the previous paper² are used.) The T_1 's in these ranges are minimal at 88°C (\uparrow) and 115°C (\uparrow). Below 115°C , T_1 increases in the order of $\gamma = 0, 90,$ and 45° , and increases in the order of $\gamma = 0, 45,$ and 90° between 115 and 127°C (\uparrow). In the \downarrow -process, T_1 decreases gradually with decreasing temperature and are minimal at 79°C (\downarrow). In the temperature range between 70 and

Table II. The temperatures of T_1 minima in P(VDF₇₂/TrFE₂₈) in the heating and cooling processes

	T_1	H^a	$\Delta\epsilon^{-1b}$	DSC ^b
$T_c(\uparrow)/^\circ\text{C}$	115	116	134	114
$T_c(\downarrow)/^\circ\text{C}$	79	80	84	75

^a Observed from the discontinuous narrowing of the NMR line width.²

^b Observed from the minimum of the reciprocal dielectric relaxation strength $1/\Delta\epsilon^7$ and the endotherm starting point on the DSC curve.⁷

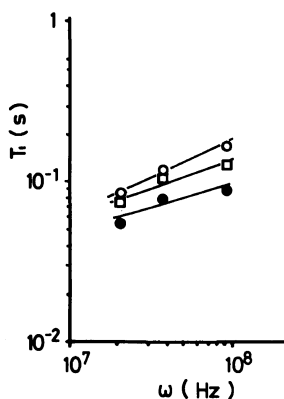


Figure 4. T_1 at 110°C in the cooling process as a function of resonance angular frequency for P(VDF₇₂/TrFE₂₈) (●, $\gamma=0^\circ$; □, $\gamma=45^\circ$, and ○, $\gamma=90^\circ$).

$65^\circ\text{C}(\downarrow)$, the T_1 increases abruptly and at $40^\circ\text{C}(\downarrow)$ returns to the value in the \uparrow -process. The β relaxation is observed slightly in the temperature region between 65 and $40^\circ\text{C}(\downarrow)$, although the T_1 minimum is not observed. The concave region with the minimum at $79^\circ\text{C}(\downarrow)$ is referred to as $\alpha_t(\downarrow)$. The T_1 values become larger in the order of $\gamma=0, 45$, and 90° in the temperature range from 127 to $75^\circ\text{C}(\downarrow)$, and $\gamma=0, 90$, and 45° below $75^\circ\text{C}(\downarrow)$. In Table I, the temperature ranges of $\beta(\uparrow)$, $\beta(\downarrow)$, $\alpha_t(\uparrow)$, and $\alpha_t(\downarrow)$ in the \uparrow - and \downarrow -processes are summarized. The temperatures of the T_1 minima in the \uparrow - and \downarrow -processes are referred to as $T_c(\uparrow)$ and $T_c(\downarrow)$, respectively, and are tabulated in Table II.

Figure 4 shows $\ln T_1$ at $110^\circ\text{C}(\downarrow)$ as a function of $\ln\omega$. The filled circle and the unfilled rectangle and circle indicate the values of T_1 for $\gamma=0, 45$, and 90° in the \downarrow -process, respectively. For each orientation, a linear relationship can be observed and the values of T_1 increase further with increasing of γ .

DISCUSSION

As shown in Table II, $T_c(\uparrow)$ and $T_c(\downarrow)$ in P(VDF₇₂/TrFE₂₈) agree approximately with the transition temperatures obtained from the dielectric,⁷ DSC⁷ and wide line NMR measurements.² This agreement may be attributed to the critical slowing down of the molecular motion near T_c^9 that the T_1 minima locate in the $\alpha_t(\uparrow)$ and $\alpha_t(\downarrow)$ regions.

Figure 5 shows the relaxation map in the \uparrow -process, where the logarithm of the relaxation frequencies ($\ln f_r$) are plotted as a dashed line against T_{-1} based on the results of the dielectric measurement for P(VDF₇₃/TrFE₂₇).¹⁰ This curve is of the Willian–Watt type which may be due to molecular motion of the chain backbone in partially crystalline regions.^{7,10} In this relaxation map, the temperatures of the line-width narrowing and the T_1 minima at $90, 36$, and 20 MHz for the β and α_t relaxation processes in P(VDF₇₂/TrFE₂₈) are also shown. (Here, the α_b relaxation process described in the previous paper² was not observed.) The NMR data for the β relaxation process locate in the neighborhood of the $\ln f_r$ vs. T^{-1} curve. While, the temperature of T_1 minimum for the α_t which are plotted as filled square is independent of the relaxation frequency. This finding also supports that the α_t relaxation process is attributed to the ferroelectric phase transition. It should be here noted that no T_1 minimum in the β -relaxation process is observed in the \downarrow -process and a discontinuity is observed in the T_1 vs. T curves at about 67°C for each orientation of the sample. The latter finding suggests that the transition from ferro- to paraelectric phase is of the first order.

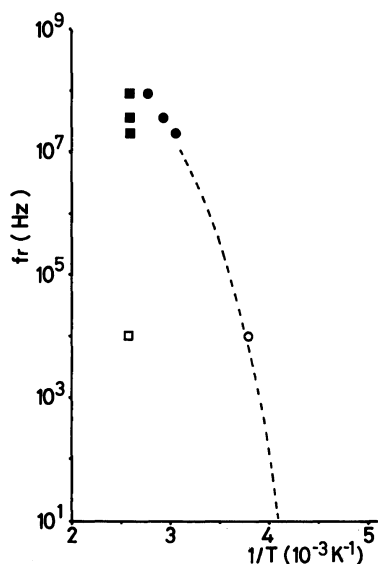


Figure 5. The relaxation map of P(VDF₇₃/TrFE₂₇) and P(VDF₇₂/TrFE₂₈) in the heating process. The dashed line (---) represents the logarithm plot of resonance frequency vs. reciprocal temperature in P(VDF₇₃/TrFE₂₇).¹⁰ The filled circles (●) and filled squares (■) indicate the temperatures of $T_{1\min}$ in P(VDF₇₂/TrFE₂₈) for β and α_1 relaxation processes, respectively. The unfilled circles (○) and squares (□) represent temperatures of the NMR line width narrowing for the β and α_1 relaxation processes in P(VDF₇₂/TrFE₂₈), respectively.²

Since the vector \vec{r}_{12} for an isolated spin pair in the chain is perpendicular to the chain axis, the β indicated in Figure 1 becomes 90° . Therefore, at the high temperature limit, $\omega\tau_D \ll 1$, eq 8 reduces to

$$\frac{1}{T_1} = A \left\{ (1 + 2\sqrt{2}) + 6 \cos^2 \gamma (1 - 2\sqrt{2}) \cos^4 \gamma \right\} \omega^{-1/2} \tau_D^{1/2} \quad (9)$$

where $A = 9/128 \gamma^4 n^2 I(I+1) r_{12}^{-6}$. Now we assume the variation of τ_D with $T(K)$, as follows:

$$\tau_D = \tau_0 \exp(\Delta E/RT) \quad (10)$$

where ΔE is the activation energy and τ_0 is the correlation time for $T = \infty$. Inserting eq 10 into

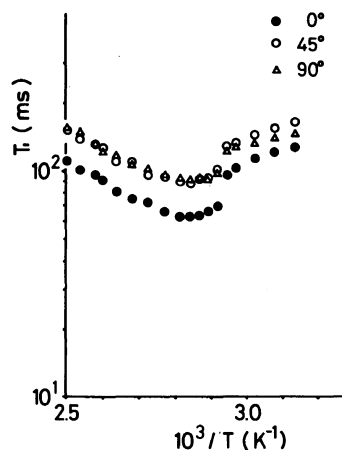


Figure 6. Plots of logarithm T_1 against reciprocal temperature for the cooling process in P(VDF₇₂/TrFE₂₈). The filled and unfilled circles, and the unfilled triangles indicate T_1 's for $\gamma = 0, 45, \text{ and } 90^\circ$, respectively.

eq 9 and taking the logarithm of both sides lead to

$$\begin{aligned} \ln T_1 = & -\frac{1}{2} \left(\frac{\Delta E}{RT} \right) + \frac{1}{2} \ln \omega - \frac{1}{2} \ln \tau_0 \\ & - \ln \left\{ (1 + 2\sqrt{2}) + 6 \cos^2 \gamma \right. \\ & \left. + (1 - 2\sqrt{2}) \cos^4 \gamma \right\} + \ln A \quad (11) \end{aligned}$$

This equation shows that in the high temperature region, the plots of the $\ln T_1$ against T^{-1} and the plots of the $\ln T_1$ against $\ln \omega$ yield straight lines with the slopes $-\Delta E/2R$ and 0.5, respectively. The plots of the $\ln T_1$ vs. T^{-1} shown in Figure 6 yield straight lines in the temperature region between 95 and 127°C (1). Then, we present here an interpretation for the experimental results for $\gamma = 0, 45, \text{ and } 90^\circ$ as follows: (i) The slope observed for the straight lines shown in Figure 4 agrees with the theoretical value, 0.5. (ii) The activation energy ΔE is determined to be $8.2 \text{ kcal mol}^{-1}$ from the slope of the straight line by using eq 11.

For certain values of ω and T (or τ_D), eq 11 predicts that T_1 takes the minimum for $\gamma = 0^\circ$ and the maximum for $\gamma = 90^\circ$. The theoretic-

cal ratios of T_1 's for $\gamma=45$ and 90° to that for $\gamma=0^\circ$ are 1.26 and 2.1, respectively. These values agree qualitatively with the averaged ratios 1.28 and 1.4 obtained from the experimental data for $\gamma=0, 45,$ and 90° at various temperatures from 95 to 127°C (\downarrow). The relaxation process due to the 1-D diffusion motion is referred to as α'_b . The temperature ranges of the α'_b relaxation in the \uparrow - and \downarrow -processes are also shown in Table I.

Thus the existence of a 1-D diffusion motion of the conformational defects in the paraelectric phase discussed in the previous paper² is verified from the agreements between the theoretical and experimental results on the spin lattice relaxation.

CONCLUSION

For the drawn film of P(VDF₇₂/TrFE₂₈), three kinds of T_1 relaxation processes of α_b , α_i , and β except α_b , which were described in the previous paper,² were observed in the temperature region between 40 and 130°C . The relaxation may be attributed to the molecular motion of the chain backbone in partially crystalline regions. The α_i relaxation was caused by a ferro-to-paraelectric phase transition of the first order. The T_1 for the α'_b relaxation in the paraelectric phase increased with increasing of ω , γ , and temperature T . On the base of Bloembergen's theory,⁶ T_1 was theoretically derived in terms of the non-exponential correlation function obtained by Hunt and Powles.⁴

The existence of a 1-D diffusion motion of the conformational defect in the paraelectric phase was confirmed by a reasonable agreement between the theoretical and the experimental results.

Acknowledgements. The authors are grateful to Dr. Hiroji Ohigashi of Engineering Research Laboratories, Toray Industries Inc., for helpful discussions, and Drs. Syun Koizumi, Junichi Sako, Toshiharu Yagi and Yoshihide Higashihata of the Daikin Kogyo Co., Ltd., for supplying samples of VDF/TrFE copolymers.

REFERENCES

1. K. Tashiro, K. Takano, M. Kobayashi, Y. Chatani, and H. Tadokoro, *Polymer*, **22**, 1312 (1981).
2. F. Ishii, A. Odajima, and H. Ohigashi, *Polym. J.*, **15**, 875 (1983).
3. R. E. Diez, F. R. Merritt, R. Dingle, D. Hone, B. G. Silibernagel, and P. M. Richards, *Phys. Rev. Lett.*, **9**, 1186 (1971).
4. B. I. Hunt and J. G. Powles, *Proc. Phys. Soc.*, **88**, 513 (1966).
5. J. G. Powles and K. Luszczynski, *Physica*, **25**, 455 (1959).
6. N. Bloembergen, *Phys. Rev.*, **104**, 1542 (1956).
7. N. Koizumi, N. Haikawa, and H. Habuta, *Ferroelectrics*, **57**, 99 (1984).
8. M. E. Rose, "Elementary Theory of Angular Momentum," John Willy & Sons, Inc., New York, London, 1961, Chapter IV.
9. T. Furukawa, G. E. Johnson, and H. E. Bair, *Ferroelectrics*, **32**, 61 (1981).
10. N. Haikawa and N. Koizumi, *Polym. Prepr., Jpn.*, **31**, 2902 (1982).